Journal of Photochemistry and Photobiology A: Chemistry 203 (2009) 155–160

Contents lists available at ScienceDirect

Journal of Photochemistry and Photobiology A: Chemistry

journal homepage: www.elsevier.com/locate/jphotochem

Dependence of photoinduced surface friction force variation on UV intensity and atmosphere in polycrystalline TiO_2 thin films

Naoki Arimitsu [a], Akira Nakajima [a,*], Toshiya Watanabe [b], Yoshikazu Kameshima [a], Kiyoshi Okada [a]

[a] Department of Metallurgy and Ceramics Science, Graduate School of Science and Engineering, Tokyo Institute of Technology, 2-12-1 O-okayama, Meguro-ku, Tokyo 152-8552, Japan
[b] Research Center for Advanced Science and Technology, The University of Tokyo, 4-6-1 Komaba, Meguro-ku, Tokyo 153-8904, Japan

ARTICLE INFO

Article history:
Received 5 August 2008
Received in revised form 18 December 2008
Accepted 14 January 2009
Available online 3 March 2009

Keywords:
Titanium dioxide
Polycrystalline thin films
Friction
Atomic force microscopy

ABSTRACT

Anatase polycrystalline thin films and a plasma crystallization process were used to investigate the dependence of the photoinduced friction force variation for a TiO_2 surface on the UV intensity and atmosphere. Photoinduced friction force variation for UV illumination time was divisible into two stages, decreasing and increasing, where the switching time between these two stages and the degree of variation depended on the UV intensity and atmosphere. The decreasing stage was attributable to the photocatalytic decomposition of organic compound adsorbed onto the surface, whereas the increasing stage was attributed to the capillary effect or an increase in the adsorbed water layer. Results demonstrated that UV intensity and atmosphere controlled the friction force.

1. Introduction

Since the discovery that TiO_2 can breakdown water, the photoinduced reaction of titanium dioxide [1] has been well studied especially the strong oxidation power of photo-generated radical species [2] for water and air purification applications [3–6]. In addition to these conventional applications, another intriguing phenomenon, i.e., the generation of a highly hydrophilic TiO_2 surface by UV illumination (photoinduced hydrophilicity) [7], was reported in the 1990s. This unique surface exhibits excellent antifogging and self-cleaning properties, which have led to TiO_2 coatings in various industrial items [8].

These unique photochemical properties might reflect the difference in other surface properties. Several scientists have reported photoinduced friction force variation on a TiO_2 surface using friction force microscopy (FFM). Wang et al. have revealed unique hydrophilic–hydrophobic domain structures on the rutile (1 1 0) face, which has oxygen bridging sites and exhibits a high hydrophilic conversion rate [7]. We have reported that UV illumination in dry air increases the friction force of the rutile (0 0 1) face as the surface negative polarization increases [9]. Sirghi et al. reported that the friction force for a highly hydrophilic polycrystalline TiO_2 film surface after UV illumination is larger than that before UV illumination [10,11], and attributed this result to the capillary water condensation effect at the tip-sample contact. However, comprehensive research on the UV intensity and atmosphere dependences of the photoinduced friction force variation on the surface of TiO_2 has yet to be conducted.

In this study, we investigate these effects using FFM. Then we discuss the relation between these changes and photocatalytic reactions. For FFM measurements, the sample surface must have a certain flatness and smoothness. Although a polished surface of a single crystal satisfies this requirement, individual differences in the photoinduced friction force variation can be considerable, probably because of fluctuations in the residual stress by the polishing process. For this study, we employed anatase polycrystalline thin films and a plasma crystallization process [12,13], which enable the crystallization of alkoxide-derived TiO_2 precursor films within 2 min with a sample temperature lower than 150 °C. Films produced using this process exhibit photoinduced hydrophilicity as well as a flatter and smoother surface than normal polycrystalline thin films from sol–gel processing and heat treatment around 500 °C.

2. Experimental

2.1. Sample preparation and characterization

A commercial titanium alkoxide solution (NDH-510C; Nippon Soda Co., Ltd., Tokyo, Japan) was spin coated onto a Si (1 0 0) substrate at 4000 rpm for 15 s, and vacuum ultraviolet light was illuminated on the film using a Xe excimer lamp (172 nm wavelength, UER20; Ushio Inc., Tokyo, Japan) for 1 h at 7 mW cm^{-2} in ambient air. Then the TiO_2 precursor films were treated with capacitively coupled RF plasma in O_2 for 2 min [13]. The crystalline phase

* Corresponding author. Tel.: +81 3 5734 2525; fax: +81 3 5734 3355.
E-mail address: anakajim@ceram.titech.ac.jp (A. Nakajima).

1010-6030/$ – see front matter © 2009 Elsevier B.V. All rights reserved.
doi:10.1016/j.jphotochem.2009.01.009

was evaluated using XRD (PW-3050; Philips Co., Amsterdam, The Netherlands) with Cu Kα radiation and a fixed X-ray incident angle of 1.0°. Film thickness and refractive index were evaluated using ellipsometry (V-VASE; J.A. Woolam Corp., Tokyo, Japan). The surface structure and roughness were evaluated using a tapping mode atomic force microscope (AFM: JSPM-5200; JEOL, Tokyo, Japan) with a Si rectangular cantilever (NSC35/C; MikroMasch, Tallinn, Estonia). The nominal spring constant was 4.5 N m^{-1}. The measurement area was a 1 μm × 1 μm region. Wettability conversion of the film by UV illumination was examined in ambient air using a contact angle meter (CA-X; Kyowa Interface Science Co., Ltd., Saitama, Japan) and a droplet size of 1.0 μL. A fluorescent black light bulb was used as the UV illumination source and the UV intensity was changed to 0.01, 0.1, and 0.5 mW cm^{-2}.

2.2. Evaluation of friction force variation under various conditions

The surface friction force was evaluated by FFM in contact mode using the same AFM with a Si_3N_4-coated Si rectangular cantilever (CSC38/A; MikroMasch, Tallinn, Estonia). The nominal spring constant was 0.08 N m^{-1}. The measurement area was 1 μm × 1 μm. The normal load was set at 10 nN. A BK7 glass cover was used to control the sample chamber atmosphere (volume of ca. 1.4 L). Under ambient air conditions (35% relative humidity, ca. 1 × 10^4 ppm H_2O content), UV with an intensity of 0.01, 0.1, or 0.5 mW cm^{-2} was illuminated on the film surface over the glass cover without introducing gas. A Hg–Xe lamp with an optical-fiber coupler was used for UV illumination, but was terminated at a set time. Then, the FFM image and contact mode AFM image were recorded simultaneously. The scanning time required for each measurement area was approximately 100 s. Alternatively, under the dry gas conditions, dry air (H_2O content of ca. 0.5 ppm; Taiyo Nippon Sanso Corp., Tokyo, Japan) or dry nitrogen (H_2O content of ca. 7 ppm; Toho Sanso Co., Ltd., Kanagawa, Japan) flowed into the sample chamber for 10 min (flow rate 2 L min^{-1}) after evacuating the chamber for 60 min by an oil-free diaphragm pump (pressure 1 kPa). Then, the FFM image was recorded with flowing dry gas (flow rate 0.5 L min^{-1}) during 0.5 mW cm^{-2} UV illumination in the same way as that in ambient air. Moreover, humidity control of the flowing air was carried out. After the FFM measurement was conducted in dry air, wet air with relative humidity of 50% flowed into the sample chamber for 10 min (flow rate: 0.5 L min^{-1}) without UV illumination. Then, UV illumination was started again under the wet air condition.

To evaluate the friction force, the histogram of each FFM image was fitted with a Gaussian function. The average and two sigma values from the function were used respectively as the average friction force and standard deviation. The water contact angles of the film before and after the FFM measurement were also measured in ambient air.

2.3. Kelvin probe force microscopy of the stearic acid coating under UV illumination

For detailed investigation of the relation between photocatalytic decomposition of surface organic compounds and friction force variation, photodegradation of stearic acid deposited onto the TiO_2 film was examined using Kelvin probe force microscopy (KFM). This organic compound was selected because of its easy oxidation and low vapor pressure. An 8.8 × 10^{-4} M methanol (Wako Pure Chemical Industries Ltd., Tokyo, Japan) solution of stearic acid ($C_{17}H_{35}COOH$, 99%; Wako Pure Chemical Industries Ltd., Tokyo, Japan) was spin coated onto the TiO_2 film at 1000 rpm for 20 s. Then the coating was dried under a stream of nitrogen. The friction force variation of the sample during 0.1 mW cm^{-2} UV illumination was evaluated using the aforementioned FFM under ambient air conditions. Under identical conditions, the surface potential was evaluated using KFM in tapping mode with the same AFM with a Ti–Pt coated Si rectangular cantilever (NSC36/C; MikroMasch, Tallinn, Estonia). The nominal spring constant was 0.6 N m^{-1}. The measurement area was a 1 μm × 1 μm region. Between the probe and sample, AC voltage of 1.8 V was applied at a frequency of 10 kHz. To evaluate the surface potential, the histogram of each KFM image was fitted with a Gaussian function. The average and two sigma values from the function were used, respectively, as the average surface potential and standard deviation.

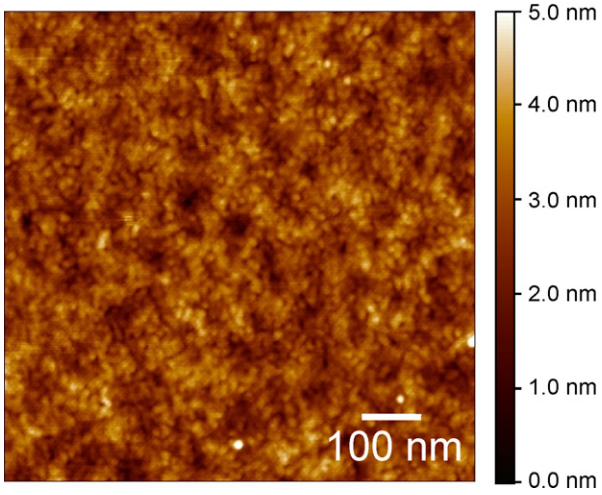

Fig. 1. Tapping mode AFM image of the TiO_2 thin film prepared using the plasma crystallization process.

3. Results and discussion

XRD measurements revealed that the film is composed solely of anatase with random crystallite orientation. Ellipsometry analysis revealed that the film is 107 nm thick with a refractive index of 2.2 at a wavelength of 550 nm. Fig. 1 shows a tapping mode AFM image of a film. The average roughness (R_a) of this film was about 0.4 nm; its surface was composed of grains of 10–20 nm diameter.

Fig. 2 depicts the average roughness of contact mode AFM images after 0.1 and 0.5 mW cm^{-2} UV illumination in ambient air

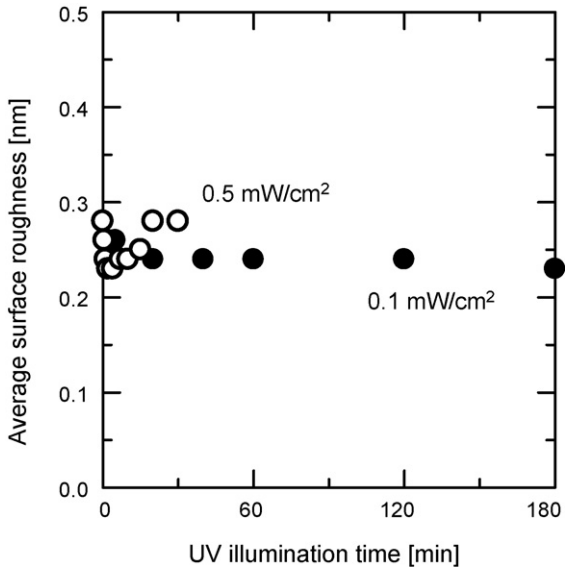

Fig. 2. Average surface roughness measured for AFM image under 0.1 and 0.5 mW cm^{-2} UV illumination in ambient air.

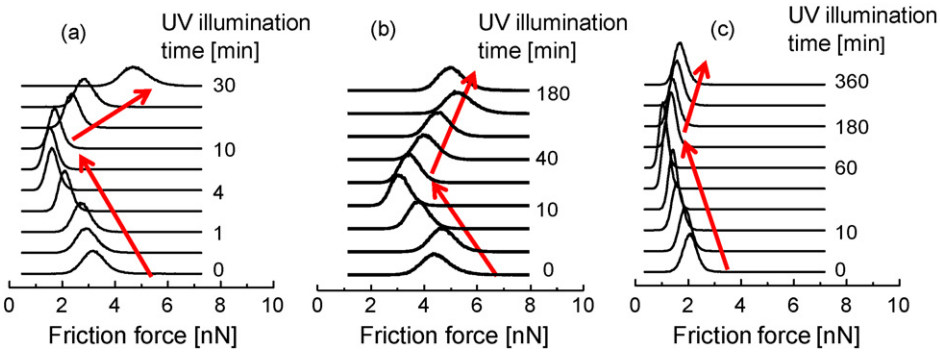

Fig. 3. UV intensity and illumination time dependences of the friction force distribution in ambient air: (a) 0.5 mW cm^{-2}, (b) 0.1 mW cm^{-2}, and (c) 0.01 mW cm^{-2}. Distribution of friction force.

for a given period. It changed slightly within 0.05 nm. Compared to former studies on the photoinduced roughness variation [14,15], the absolute value of variation was less marked in this film (in the former research, the value was 0.2–0.5 nm). Because the AFM image is often blurred during the photoinduced surface roughness variation of anatase polycrystalline films (probably because of the continuous surface roughness change, and image blurring was not observed from the sample in this study) [14,15], it remains unclear whether the difference of the absolute value of the roughness variation is meaningful. However, two differences pertain in the present research: the UV intensity and sample. The UV intensity used in this study is less than that used previously (0.7 mW cm^{-2}), and the sample is prepared under low processing temperature in the plasma process and the resultant fine microstructure in the film. Detailed analysis of the effects of these factors on the trend of photoinduced surface roughness variation is a subject for future work.

Fig. 3 shows the UV intensity and illumination time dependences of the friction force distribution in ambient air. Fig. 4 portrays the relation between the average friction force and water contact angle variations in ambient air. In all figures, the friction force initially decreased with increasing UV illumination time, but after a certain period of UV illumination, the friction force began to increase. The degree of the friction force variation and the switching time depended on the UV intensity. The saturated value for the water contact angle also depended on the UV intensity. Interestingly, the switching time almost corresponded to that when the water contact angle decreased and reached its saturated value. The high UV intensity induced a large friction force variation and a low saturated value for the water contact angle. These results suggest that the photoinduced friction force variation is related to the photoinduced hydrophilicity.

The initial value difference of the friction force depends on: (a) differences in the amounts and variety of stains on the film surface during ambient air exposure, and (b) adjustment of the FFM facility (such as cantilever exchange or adjustment of the laser irradiation position to the cantilever). These factors probably cause the difference of the initial surface friction values depicted in Figs. 3 and 4.

Although temperature changes before and after FFM measurements were not evaluated in this study, we believe that they were quite small: certainly less than 10 °C. The sample was not warm even after 6 h UV illumination under 0.01 mW cm^{-1}. We make this inference because: (a) the film thickness is ca. 100 nm, whereas the substrate is Si of 0.5 mm thickness; (b) the sample stage of the probe microscope is metal, and the heat capacity of the facility is quite large; (c) UV was illuminated with low intensity.

Fig. 5 presents average friction force variations during 0.5 mW cm^{-2} UV illumination under various atmospheres. The initial decrease in the friction force during UV illumination for 30 min under dry gas conditions was not so remarkable compared to that observed in ambient air. The friction force increased gradually as the UV illumination time increased in dry air, although it remained constant in dry N_2. Moreover, after FFM measurements in ambient air and dry air, the water contact angle decreased to less than 10° and about 20° (the initial value was greater than 60°), respectively. In dry N_2, the contact angle did not decrease after the measurement. Additional experiments revealed that the results from the dry N_2 atmosphere are the same as those under wet N_2 at a relative humidity of 50%.

Fig. 6 shows the average friction force variation by changing humidity and UV illumination. When UV illumination was carried out in dry air (0–360 min), the friction force was small and almost constant. Once wet air at a relative humidity 50% flowed without UV illumination (thinly hatched area), the friction force increased gradually. When UV was illuminated in the wet air (darkly hatched area), it increased further. These results demonstrate that the friction force increase is dependent on the humidity, and that UV illumination on the surface of TiO_2 enhances this effect.

The photoinduced friction force variation in ambient air was divided into two stages: decreasing (low hydrophilic) and increasing (highly hydrophilic) ones. Under ambient air conditions, both water and organic contaminants such as hydrocarbons were present in the atmosphere and on the film surface. Figs. 7 and 8 show the average friction force by FFM and surface potential variations by KFM on the stearic acid coated film under 0.1 mW cm^{-2} UV illumination in ambient air. The friction force decreased as the UV illumination time increased, although the surface potential increased. Sugimura et al. [16] and Suzuki et al. [17] examined the SiO_2 exposed regions in octadecyltrimethoxysilane or heptadecafluorodecyltrimethoxysilane coatings by using KFM, and reported that hydrophilic regions have a higher surface potential than the surrounding hydrophobic regions. Based on these results, it is presumed that the photocatalytic decomposition of organic contaminants advances during UV illumination in the decreasing stage of friction force. The influence of organic contaminants decreased gradually, which engenders the reduced cohesive force at the tip-sample. The decreased friction force in this stage is attributable to the increased hydrophilic region, where thin water layer will be formed. This thin water layer acts as a lubricant [18–22] and gradually increases during UV illumination.

On the other hand, the increased friction force by UV illumination is observed in the highly hydrophilic stage. Existence of water molecules in the atmosphere is a key factor, as shown in Fig. 6. This change is attributed to three phenomena: surface roughness variation, water condensation at the tip-sample contact, and the increase of water layer thickness. However, the surface roughness variation does not increase over the long UV illumination period (see 0.1 mW cm^{-2} case in Fig. 2). Consequently, it is presumed that the friction force increase is attributable to either water condensation or the increase of water layer thickness, or both. The effect of water condensation at the tip-sample contact, with its resulting

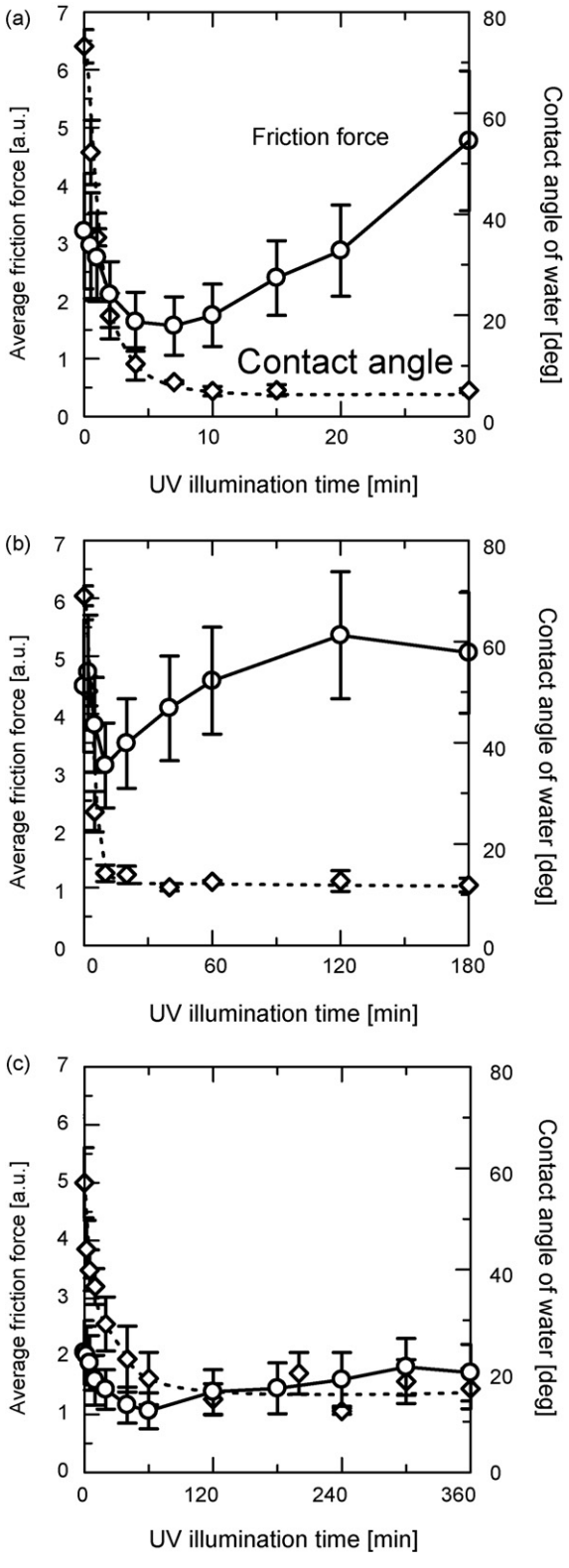

Fig. 4. UV intensity and illumination time dependences of the average friction force and water contact angle variations in ambient air: (a) 0.5 mW cm^{-2}, (b) 0.1 mW cm^{-2}, and (c) 0.01 mW cm^{-2}.

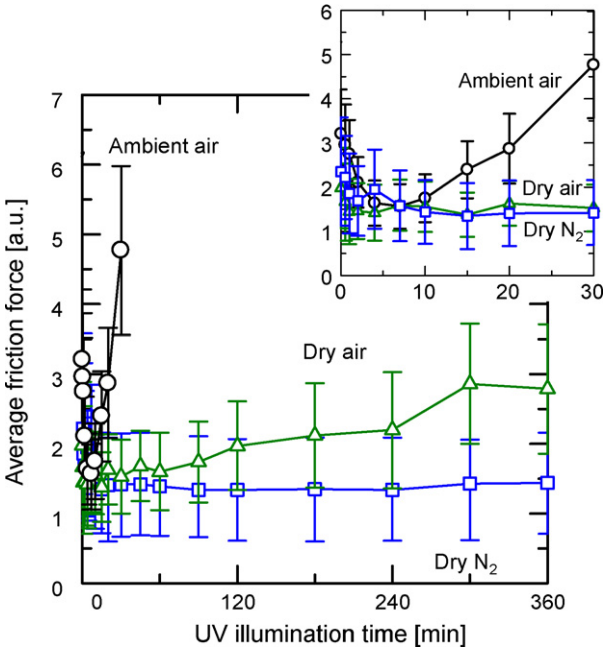

Fig. 5. Average friction force variations under 0.5 mW cm^{-2} UV illumination in various atmospheres. The inset shows expanded data for the initial 30 min.

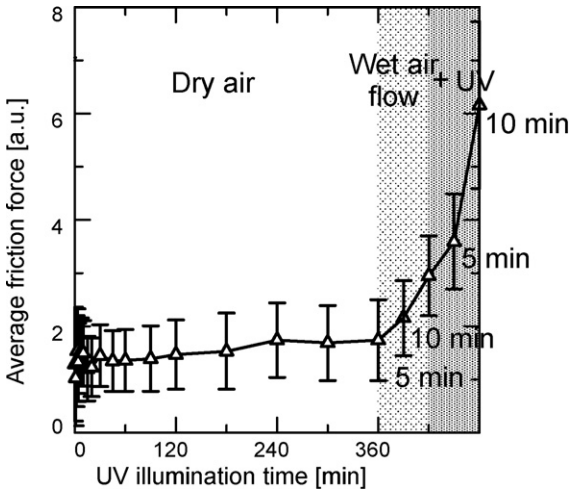

Fig. 6. Average friction force variation upon 0.5 mW cm^{-2} UV illumination from under dry air to wet air at relative humidity of 50%. The thinly hatched area shows the duration of flowing wet air without UV illumination. The darkly hatched area shows the duration of flowing wet air with UV illumination.

capillary effect of the water layer has been pointed out by several investigations [10–11,21,23,24]. Meanwhile, it is inferred that the excess increase of the surface water layer thickness might lead to increased moving resistance of the cantilever. Further detailed experiments by controlling adsorption state of water molecules on TiO_2 surface are required to investigate the contribution of these two factors to the entire increase of friction force under UV illumination.

The photo-generated electron transfer from TiO_2 to oxygen is feasible considering coexisting water molecules [25], although it is difficult under dry conditions. Therefore, the coexistence of oxygen and water in the atmosphere plays an important role in the photocatalytic oxidation efficiency. Under dry air conditions, the friction force did not decrease markedly after UV illumination for 30 min. In this case, as suggested by the low initial friction force, the degree of initial contamination on the surface was less than the ambient air condition because of prior vacuum pumping and the continuous flow of clean dry gas. Therefore, the effect of photocatalytic oxidation is less remarkable. Fig. 9 presents average friction force variations of the film with stearic acid coating under 0.5 mW cm^{-2} UV illumination in dry air. In this case, stearic acid coated onto the

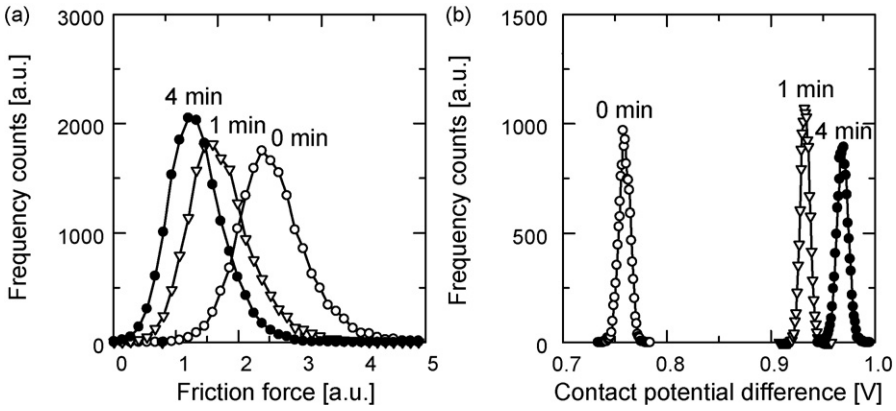

Fig. 7. Distributions of friction force and surface potential on a stearic acid coated film under 0.1 mW cm^{-2} UV illumination in ambient air: (a) friction force, and (b) surface potential.

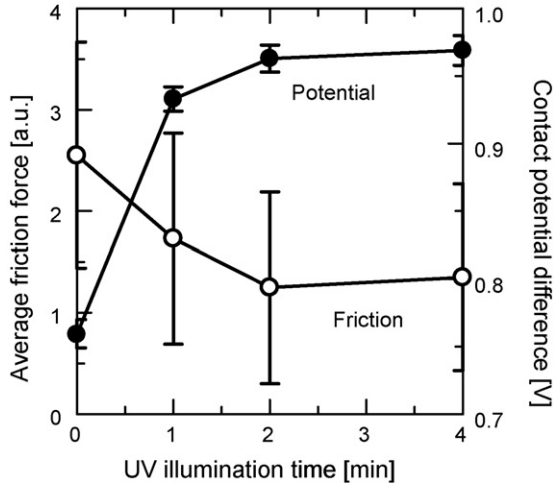

Fig. 8. Average friction force and surface potential variations on a stearic acid coated film under 0.1 mW cm^{-2} UV illumination in ambient air.

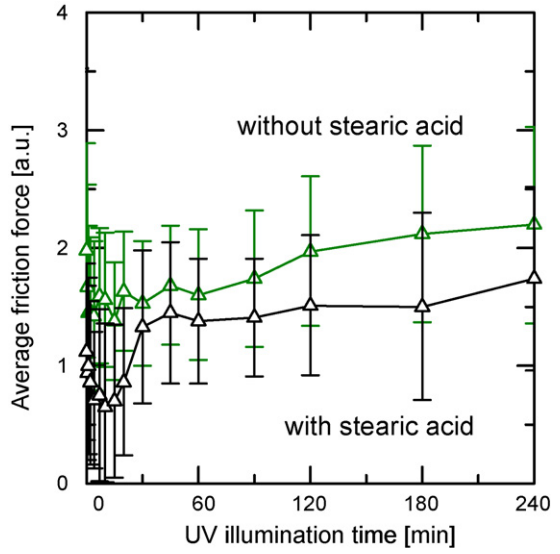

Fig. 9. Average friction force variations on the film with or without stearic acid coating under 0.5 mW cm^{-2} UV illumination in dry air.

surface will not be removed easily by prior vacuum pumping. Therefore, because of photocatalytic decomposition, the friction force initially decreased with increasing UV illumination time even in dry air. After a certain period of UV illumination, the friction force began to increase, similarly to the trend on the film without stearic acid coating. The gradual increase in the friction force under the dry air condition is attributed to the capillary effect or the increase the thickness of surface water layer, similar to ambient air. Despite the low water adsorption, deposits appear to be stable and not evaporate spontaneously [20,26]. The photocatalytic reaction does not advance in N_2 because of the impossibility of electron transfer from TiO_2 [27]. Therefore, friction force variation was not observed in the atmosphere.

In the decreasing stage, the photoinduced hydrophilicity by photocatalytic decomposition of surface organic contaminants [28–30] contributed to photoinduced friction force variation. However, the friction force started to increase and continued increasing even upon weak UV illumination after reaching a certain contact angle saturation, suggesting that continuous UV illumination increases the amount of water even after reaching a constant surface concentration of organic compounds. The possibility of a contribution of surface structural change that is amenable to formation of a thick water adsorption layer by UV illumination [31] in this stage is undeniable.

Results of the present study demonstrated that UV intensity and the atmosphere could control a relation between the photocatalytic decomposition, photoinduced hydrophilicity, and photoinduced friction force variation. The photoinduced friction force variation obtained from anatase polycrystalline thin films examined in this study is more remarkable than that of a rutile single crystal [9]. This result suggests several possibilities: (a) contribution of grain boundary [32], (b) large anisotropy in the degree of friction force variation, and (c) the effect of residual stress introduced by surface polishing or thermal treatment. The contribution of these factors is addressed to future works.

4. Conclusion

The effects of UV intensity and atmosphere on the photoinduced friction force variation for the surface of anatase polycrystalline films were investigated. The photoinduced friction force variation is divisible into decreasing and increasing stages where the switching time for these two stages and the degree of variation depends on the UV intensity and atmosphere. The decreasing stage is attributed to the photocatalytic decomposition, whereas the increasing stage is attributed to the capillary effect or the increased adsorbed water layer. These findings suggest a relation between the photocatalytic decomposition, photoinduced hydrophilicity, and photoinduced friction force variation is controllable by UV intensity and atmosphere.

Acknowledgement

This work was supported in part by a JSPS Fellowship for Young Scientists: H20-9886.

References

[1] A. Fujishima, K. Honda, Nature 238 (1972) 37–38.
[2] T. Kawai, T. Sakata, Nature 286 (1980) 474–476.
[3] D.F. Ollis, H. Al-Ekabi (Eds.), Photocatalytic Purification and Treatment of Water and Air, Elsevier, Amsterdam, London, New York, Tokyo, 1993, p. 747.
[4] I. Rosenberg, J.R. Brock, A. Heller, J. Phys. Chem. 96 (1992) 3423–3428.
[5] N. Takeda, T. Torimoto, S. Sampath, S. Kuwabata, H. Yoneyama, J. Phys. Chem. 99 (1995) 9986–9991.
[6] M.R. Hoffmann, S.T. Martin, W. Choi, D.W. Bahnemann, Chem. Rev. 95 (1995) 69–96.
[7] R. Wang, K. Hashimoto, A. Fujishima, M. Chikuni, E. Kojima, A. Kitamura, T. Shimohigoshi, T. Watanabe, Nature 388 (1997) 431–432.
[8] A. Fujishima, K. Hashimoto, T. Watanabe, TiO_2 Photocatalysis: Fundamentals and Applications, BKC Inc., Tokyo, 1999, p. 66.
[9] A. Nakajima, A. Nakada, N. Arimitsu, Y. Kameshima, K. Okada, Mater. Lett. 62 (2008) 1319–1321.
[10] L. Sirghi, T. Aoki, Y. Hatanaka, Thin Solid Films 422 (2002) 55–61.
[11] L. Sirghi, T. Aoki, Y. Hatanaka, Surf. Rev. Lett. 10 (2003) 345–349.
[12] H. Ohsaki, Y. Shibayama, A. Nakajima, A. Kinbara, T. Watanabe, Thin Solid Films 502 (2006) 63–66.
[13] N. Arimitsu, A. Nakajima, Y. Kameshima, Y. Shibayama, H. Ohsaki, K. Okada, Surf. Coat. Technol. 201 (2006) 3038–3043.
[14] K. Katsumata, A. Nakajima, T. Shiota, N. Yoshida, T. Watanabe, Y. Kameshima, K. Okada, J. Photochem. Photobiol. A 180 (2006) 75–79.
[15] N. Arimitsu, A. Nakajima, K. Katsumata, T. Shiota, T. Watanabe, N. Yoshida, Y. Kameshima, K. Okada, J. Photochem. Photobiol. A 190 (2007) 53–57.
[16] H. Sugimura, K. Hayashi, N. Saito, N. Nakagiri, O. Takai, Appl. Surf. Sci. 188 (2002) 403–410.
[17] S. Suzuki, A. Nakajima, N. Yoshida, M. Sakai, A. Hashimoto, Y. Kameshima, K. Okada, Langmuir 23 (2007) 8674–8677.
[18] L. Xu, H. Bluhm, M. Salmeron, Surf. Sci. 407 (1998) 251–255.
[19] J. Hu, X.D. Xiao, D.F. Ogletree, M. Salmeron, Surf. Sci. 327 (1995) 358–370.
[20] A.A. Feiler, P. Jenkins, M.W. Rutland, J. Adhes. Sci. Technol. 19 (2005) 165–179.
[21] W. Karino, H. Shinbo, Tribol. Int. 40 (2007) 1568–1573.
[22] R.R.M. Zamora, C.M. Sanchez, F.L. Freire Jr., R. Prioli, Phys. Status Solidi (a) 201 (2004) 850–856.
[23] A. Opitz, S.I.U. Ahmed, J.A. Schaefer, M. Scherge, Surf. Sci. 504 (2002) 199–207.
[24] J.N. Israelachvili, Intermolecular and Surface Forces: With Applications to Colloidal and Biological Systems, Academic Press, London, Orlando, San Diego, New York, Toronto, Montreal, Sydney, Tokyo, 1985, p. 222.
[25] Y. Nosaka, A. Nosaka (Eds.), Nyumon Hikari Shokubai, Tosho Press, Tokyo, 2004, pp. 63–87 (in Japanese).
[26] S. Rozhok, P. Sun, R. Piner, M. Lieberman, C.A. Mirkin, J. Phys. Chem. B 108 (2004) 7814–7819.
[27] W.M. Latimer, The oxidation states of the elements and their potentials in aqueous solutions, Prentice-Hall Inc., New York, 1952, pp. 48, 102.
[28] M. Takeuchi, K. Sakamoto, G. Martra, S. Coluccia, M. Anpo, J. Phys. Chem. B 109 (2005) 15422–15428.
[29] C.Y. Wang, H. Groenzin, M.J. Shultz, Langmuir 19 (2003) 7330–7334.
[30] T. Zubkov, D. Stahl, T.L. Thompson, D. Panayotov, O. Diwald, J.T. Yates, J. Phys. Chem. B 109 (2005) 15454–15462.
[31] N. Sakai, A. Fujishima, T. Watanabe, K. Hashimoto, J. Phys. Chem. B 107 (2003) 1028–1035.
[32] K. Katsumata, A. Nakajima, H. Yoshikawa, T. Shiota, N. Yoshida, T. Watanabe, Y. Kameshima, K. Okada, Surf. Sci. 579 (2005) 123–130.